Discovery of novel acylguanidine-based small molecules that block Influenza A M2 ion channel activity and drug-resistant virus

Ian Tietjen [1], Scott C. Miller [1], Hannah E. Boycott [1], Jodene Eldstrom [1], Daniel C. Kwan [1], Doug Chou [1], Pouria Jalily [1], Daniel Menconda [1], F. Brent Johnson [2], Michaela Schmidtke [3], David D. Busath [2], David Fedida [1]

[1]University of British Columbia, Vancouver, BC, Canada; [2]Brigham Young University, Provo, UT, United States; [3]Jena University Hospital, Jena, Germany.

Background

The emergence of drug-resistant influenza highlights an urgent and unmet need for new antivirals. Amantadine and rimantadine are historically potent antivirals that inhibit the M2 ion channel of influenza A virus; however, the M2 Ser31Asn (S31N) polymorphism has become so prevalent that these adamantanes are no longer recommended for clinical use [1]. While numerous adamantane derivatives have been synthesized in an effort to identify M2(N31) inhibitors, few of these derivatives confer significant M2(N31) blockade or antiviral activity, highlighting the need to pursue alternative chemical scaffolds. Here we describe a series of novel acylguanidine-based small molecules that are potent inhibitors of the M2 viral ion channel, as measured by whole-cell patch clamp electrophysiology, and influenza viruses, as measured by both miniplaque and standard viral plaque assays.

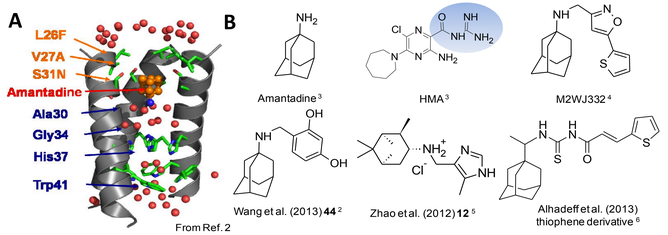

Figure 1. M2 viral ion channel and reported inhibitors. A, M2 tetramer plus amantadine. Drug-resistance mutations include L26F, V27A, S31N, A30T, and G34E [2]. Only L26F, V27A, and S31N are found in the wild, with S31N in >90% of resistant strains [1]. His37 is a proton sensor, and Trp41 is a selectivity filter that confers unidirectional ion currents. **B,** structures of some reported M2 inhibitors [2-6]. Blue, acylguanidine moiety. **C,** M2 inhibitor activities.

C

Compound	Ref.	Assay	M2 genotype	Activity
Amantadine	2	Two electrode voltage clamp (TEVC, M2 expressed in *Xenopus* oocytes)	S31	IC50 = 16.1uM
	3	Yeast growth restoration	S31	EC50 = 0.1 μM
HMA	2	TEVC	N31	IC50 = 200 μM
	3	TEVC	S31	90% block at 100 μM
		Yeast growth restoration	S31	EC50 = 1.1 uM
M2WJ332	4	TEVC	S31	11% block at 100 μM
			N31	IC50 = 16 μM
44	2	TEVC	S31	IC50 = 59 μM
			N31	IC50 = 35.2 μM
12	5	Whole-cell patch clamp	S31	96% block at 100 μM
			N31	27% block at 100 μM
Thiophene derivative	6	Bacterial growth restoration	N31	EC50 = 25 μM

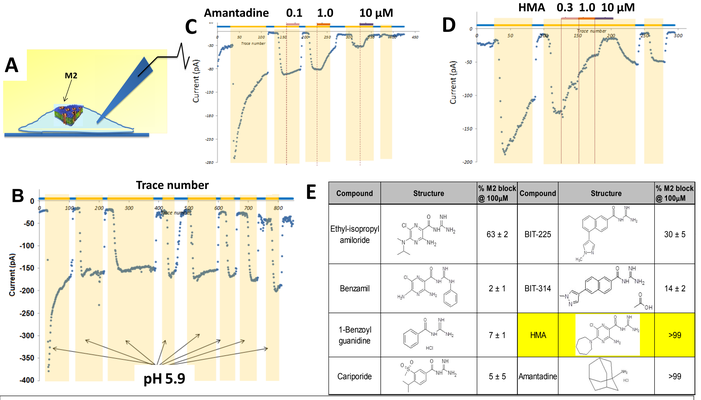

Figure 2. Identification of HMA as a potent M2 inhibitor. A, HEK cells expressing Influenza A M2 (H9N2, S31) are assessed for pH-dependent electrical currents by whole-cell patch clamp electrophysiology. **B,** Representative diary plot of pH-dependent M2 current. Cells are cultured at pH 7.4 (blue bars), and M2 currents are reversibly activated by perfusion of extracellular pH 5.9 (orange bars and shading). Cells are held at -40 mV, and 100 ms pulses of -80 mV are recorded every 4s (blue dots and traces). Both amantadine **(C)** and HMA **(D)** inhibit M2 currents. **E,** Percent M2 current block by 100 μM of acylguanidine-based molecules.

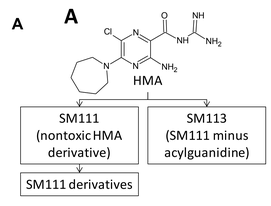

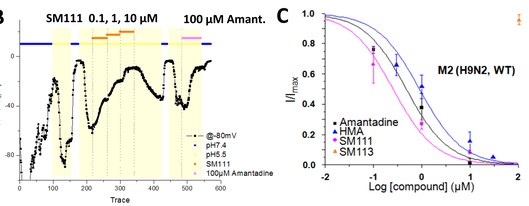

Figure 3. Identification of HMA derivatives with limited cytotoxicity. A, Strategy to synthesize novel HMA derivatives. **B,** Representative diary plot of M2(S31) currents plus SM111. **C,** Dose-dependent inhibition of M2(S31) currents by amantadine, HMA, SM111, and SM113. **D**, HEK cell survival, as measured by MTT assay, after 24h treatment with listed compounds. **E**, Inhibition of hERG ion channel by compounds, as measured by whole-cell patch clamp.

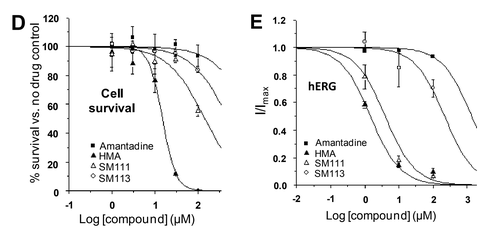

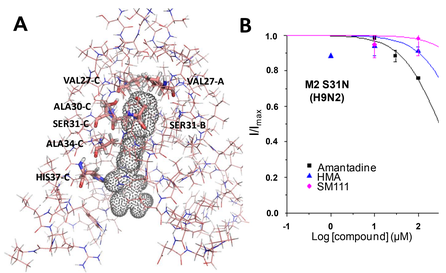

Figure 4. SM111 and amantadine inhibit M2 by similar mechanisms. A, Model of SM111 interacting with the transmembrane residues of M2(S31) (PDB entry 3C9J; residues 22-46 of M2 of A/Hong Kong/156/97(H5N1)). Modeling was performed using Autodock 4.2 [10] and assumed a rigid M2 structure with 4 flexible residues per subunit (V27, S31, I33, H37). The lowest energy configuration and interacting residues (+ subunit A-D) are shown. **B**, Amantadine, HMA, and SM111 all have reduced blockade of amantadine-resistant H9N2 M2(N31) currents. **C-E,** Diary plots of normalized M2(S31) currents plus 10 μM amantadine (**C**), SM111 (**D**), or SM111 followed by amantadine (**E**). Amantadine does not displace SM111, indicating that both compete to inhibit M2(S31).

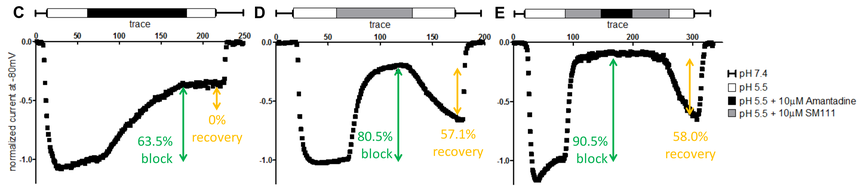

Parameter	M2 (Wild-type) block		M2 (N31) block	Cell survival		hERG block	
Assay	Electrophysiology		Electrophysiology	MTT assay		Electrophysiology	
Measure	% block at 100 μM ± SEM	IC50 (μM)	% block at 100 μM ± SEM	CC_{50} (μM)	SI	IC_{50} (μM)	SI
Amantadine	>99	0.6 ± 0.2	24 ± 1	>100		>100	
HMA	>99	1.3 ± 0.3	10 ± 3	16 ± 1	12.3	1.5 ± 0.1	1.2
SM111	**>99**	**0.2 ± 0.1**	**<10**	**130 ± 10**	**650**	**3.2 ± 0.8**	**16.0**
SM109	<10						
SM117	<10		<10				
SM112	16 ± 4		15				
SM113	<10		<10				
SM116	36 ± 3						
SM114	>99	0.4 ± 0.1	<10	19 ± 1	47.5	5.6 ± 0.4	14.0
SM118	>99	5.0 ± 1.0		24 ± 1	4.8	5.0 ± 2.0	1.0
SM120	56 ± 2	50 ± 1	<10	39 ± 1	0.8	22 ± 3	0.4
SM102	33 ± 8						
SM107	33 ± 5						
SM119	33 ± 3		<10				
DC100	15		16 ± 4				
SM124	>99	1.8 ± 0.0	10 ± 8	62 ± 6		1.9 ± 0.4	1.1
SM123	15 ± 24		<10				
SM122	**<10**		**32 ± 17**	**85 ± 6**		**5.9 ± 0.2**	

Figure 5. Properties of novel HMA derivatives.

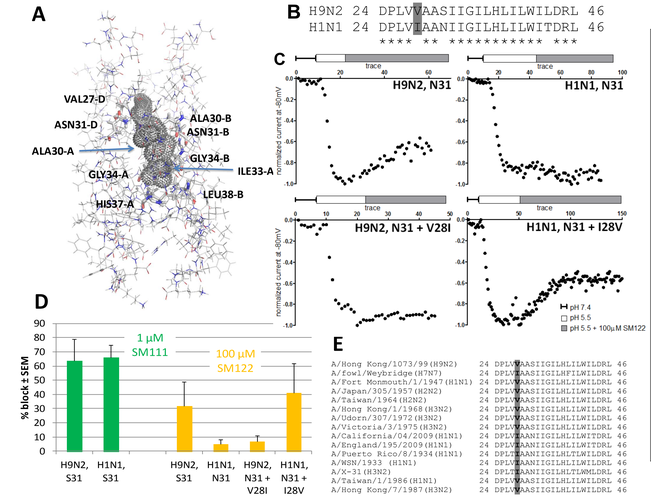

Figure 6. SM122 block of M2(N31) currents is dependent on Val28. A, Lowest-energy configuration of SM122 interacting with M2(N31) (PDB entry 2ly0; residues 19-49 of M2 of A/Chiba/5/71(H3N2)) [4]. Modeling assumed a rigid M2 structure with 4 flexible residues per subunit (V27, N31, I33, H37) plus W41 in Subunit A. **B**, Sequence alignment of transmembrane domains from H9N2 and H1N1 M2(N31) sequences. **C**, Representative diary plots of currents from various M2(N31) sequences with Val28 or Ile28, plus SM122. **D,** Effects of SM111 and SM122 on M2 currents. SM122 does not block currents from M2(N31) sequences containing Ile28. **E,** Alignment of M2 transmembrane domains from various influenza A strains, showing that Val28Ile is well tolerated.

Assay	Virus	Genotype	EC50 (μM) ± SEM		
			Amantadine	SM111	SM122
Mini-plaque	A2/Taiwan/1/1964 (H2N2)	V28 + S31	**0.34 ± 0.01**	**13 ± 0.3**	43 ± 7
	A/Victoria/3/1975 (H3N2)	V28 + S31	**2.8 ± 0.3**	**7.2 ± 12**	46 ± 4
	A/WSN/1933 (H1N1)	I28 + N31	24 ± 1	>80	>80
	A/California/04/2009 (H1N1)	I28 + N31	>80	>80	**10.4 ± 0.2**
	A/PR/8/1934 (H1N1)	T27 + I28 + N31	24 ± 4	21 ± 2	**2.4 ± 0.5**
Cytopathic effect	A/WSN/1933 (H1N1)	I28 + N31	>80	40 ± 13	>80
	A/WSN/1933 (H1N1), N31S	I28 + S31	**0.4 ± 0.1**	**5.2 ± 0.3**	>80

Figure 7. Antiviral activities of SM111 and SM122. Antiviral activity of SM111 is dependent on an M2(S31) genotype, consistent with electrophysiology. In contrast, SM122 inhibits two influenza stains expressing M2(N31 + *I28*), indicating that SM122 can block influenza A replication via an alternative mechanism.

Summary

- SM111 is a novel acylguanidine-based small molecule with improved M2(S31) blockade, reduced cytoxicity, and reduced hERG blockade compared to HMA.
- Molecular modeling and electrophysiolgical studies suggest that SM111 competes with amantadine for M2(S31) block. No derivatives were synthesized with improved activity against M2(S31).
- SM111 does not inhibit adamantane-resistant M2(N31). In contrast, SM122 has limited but significant activity against M2(N31), but only in the presence of a V28 polymorphism, indicating V28I as a novel modifier of M2 inhibitor efficacy.
- In viral culture, SM111 inhibits M2(S31) but not M2(N31) encoding viruses, consistent with electrophysiology data.
- Surprisingly, SM122 inhibits some M2(N31 + I28)-encoding viruses, suggesting that SM122 is able to block influenza A replication by an alternative mechanism.
- Taken together, we identify new prototypes for future inhibitors of drug-resistant influenza.

References

1. Bright et al., *Lancet* 366:1175-1181, 2005.
2. Wang et al., *J Med Chem* 56:2804-2812, 2013.
3. Balgi et al., *PLoS ONE* 8:e55271, 2013.
4. Wang et al., *PNAS* 110:1315-1320, 2013.
5. Zhao et al., *Antivir Res* 96:91-99, 2012.
6. Alhadeff et al., *Biochim Biophys Acta* 1838:1068-1073, 2014.
7. Kwan et al., *Biophys J* 90:1212-1222, 2006.
8. Pinto et al., *Cell* 69:517-528, 1992.
9. Chizhmakov et al., *J Physiol* 494.2:329-336, 1996.
10. Morris et al., *J Comput Chem* 16:2785-2791, 2009.

Acknowledgements

This work is supported by a CIHR collaborative research grant partnered with Cardiome Pharma Corp (to D.F). I.T. thanks the ICAR organizers for a Travel Award

THE UNIVERSITY OF BRITISH COLUMBIA

CIHR IRSC Canadian Institutes of Health Research / Instituts de recherche en santé du Canada

ISAR INTERNATIONAL SOCIETY FOR ANTIVIRAL RESEARCH

CARDIOME PHARMA CORP.